Biochimica et Biophysica Acta 1838 (2014) 1406–1411

Contents lists available at ScienceDirect

Biochimica et Biophysica Acta

journal homepage: www.elsevier.com/locate/bbamem

Can pyrene probes be used to measure lateral pressure profiles of lipid membranes? Perspective through atomistic simulations

Miroslava Dékány Fraňová [a], Ilpo Vattulainen [b,c], O.H. Samuli Ollila [d,*]

[a] Department of Chemical Physics and Optics, Faculty of Mathematics and Physics, Charles University, Ke Karlovu 3, Prague 2 CZ-12116, Czech Republic
[b] Department of Physics, Tampere University of Technology, P.O. Box 692, FI-33101 Tampere, Finland
[c] MEMPHYS — Center for Biomembrane Physics, University of Southern Denmark, Odense, Denmark
[d] Helsinki Biophysics and Biomembrane Group, Department of Biomedical Engineering and Computational Science, Aalto University, Espoo, Finland

ARTICLE INFO

Article history:
Received 18 October 2013
Received in revised form 7 January 2014
Accepted 30 January 2014
Available online 7 February 2014

Keywords:
Lipid bilayer
Lateral pressure profile
Molecular dynamics simulation
Di-pyrenyl-phosphatidylcholine

ABSTRACT

The lateral pressure profile of lipid bilayers has gained a lot of attention, since changes in the pressure profile have been suggested to shift the membrane protein conformational equilibrium. This relation has been mostly studied with theoretical methods, especially with molecular dynamics simulations, since established methods to measure the lateral pressure profile experimentally have not been available. The only experiments that have attempted to gauge the lateral pressure profile have been done by using di-pyrenyl-phosphatidylcholine (di-pyr-PC) probes. In these experiments, the excimer/monomer fluorescence ratio has been assumed to represent the lateral pressure in the location of the pyrene moieties. Here, we consider the validity of this assumption through atomistic molecular dynamics simulations in a DOPC (dioleoylphosphatidylcholine) membrane, which hosts di-pyr-PC probes with different acyl chain lengths. Based on the simulations, we calculate the pyrene dimerization rate and the lateral pressure at the location of the pyrenes. The dimerization rates are compared with the results of di-pyr-PC probes simulated in vacuum. The comparison indicates that the lateral pressure is not the dominant determinant of the excimer/monomer fluorescence ratio. Thus, the results do not support the usage of di-pyr-PC molecules to measure the shape of the lateral pressure profile. We yet discuss how the probes could potentially be exploited to gain qualitative insight of the changes in pressure profile when lipid composition is altered.

1. Introduction

Membrane elasticity has gained a lot of attention in cell membrane biophysics, since it, for example, explains various vesicular morphologies [1] and plays a role in membrane protein functionality [2,3]. Membrane elasticity emerges from the interactions that take place within a membrane. More precisely, it has been shown how membrane elastic coefficients can be derived from the lateral pressure profile that describes how the pressure is distributed inside a lipid membrane [4,5]. Therefore, it is not surprising that the connection between membrane elasticity and membrane protein functionality has also been derived by the lateral pressure concept [6,7]. Yet, there is still room for further development, since for a mechanosensitive channel and similar proteins, the second order elasticity theory seems to be too simple to describe the dependence of functionality on membrane physical properties [8]. Further, there is still critical discussion taking place concerning the relation between the lateral pressure profile and the elastic properties of membranes [9,10].

To analyze how much the lateral pressure profile contributes to the free energy of protein activation (inducing a shift in its conformational state), two characteristics are needed [6–8]: the cross-sectional area of a membrane protein in its active and inactive states, and the lateral pressure profile in the membrane surrounding the protein. Both of these quantities are difficult to measure. As for the cross-sectional area, one needs to know the 3D structure of the membrane protein in both of its two states [8]. Though considerable progress has been made, the structure determination is still a major challenge [11]. Regarding the second case, there is no generally accepted experimental method to measure the lateral pressure profile (see below).

Given the above concerns, there are still fundamental issues to be solved before the importance of the lateral pressure profile in modulating membrane protein function can be assessed quantitatively.

Lateral pressure profiles have been calculated from various molecular dynamics simulation models with numerous lipid compositions [12,13]. On the experimental side, the situation is more difficult, since currently only one technique has been used to measure the transmembrane distribution of pressure inside lipid membranes. The technique [14] is based on the assumption that the measured excimer/monomer fluorescence ratio of di-pyrenyl-phospatidylcholine (di-pyr-PC) probes correlates with the magnitude of lateral pressure in the location of the pyrene moiety. The experiments have been used to extract two different kinds of information about the lateral pressure profile. First, for a fixed lipid bilayer system, one measures the excimer/monomer fluorescence

* Corresponding author.
E-mail address: samuli.ollila@aalto.fi (O.H. Samuli Ollila).

0005-2736/$ – see front matter © 2014 Elsevier B.V. All rights reserved.
http://dx.doi.org/10.1016/j.bbamem.2014.01.030

ratio with several di-pyr-PC probes with different acyl chain lengths [14]. In the second setup, the excimer/monomer fluorescence ratio is determined for a di-pyr-PC with a certain chain length, but here the experiments are done in lipid bilayers with different lipid compositions [15–17,14,18–20]. In the first case, the objective is to measure the shape of the lateral pressure profile, while in the latter case the aim is to measure the changes in the lateral pressure profile due to changes in lipid composition. The appropriateness of the latter measurement is supported by the increasing excimer/monomer fluorescence ratio with increasing lateral pressure (and vice versa) in phosphatidylcholine vesicles [21]. On the other hand, the decreasing excimer/monomer fluorescence ratio with increasing hydrostatic pressure has been interpreted in terms of free volume and molecular conformations, instead of lateral pressure [22,17,16,23]. Thus, currently it is not really clear whether the pyrene-based approach is appropriate for the determination of the lateral pressure profile inside lipid membranes.

In this work, our objective is to clarify this issue. We use atomistic molecular dynamics simulations to estimate the relative excimer/monomer fluorescence ratios in lipid bilayers, where some of the lipids are probes with pyrene moieties attached to varying positions in the chains of the host lipids. These simulations are compared to the simulations of probes in vacuum to separate the effect of the internal molecular conformations of di-pyr-PC and the properties of the surrounding lipid bilayer to the estimated relative excimer/monomer fluorescence ratio. Also the lateral pressure profile determined by using the approach suggested in Ref. [14]. is compared to the lateral pressure profiles calculated directly from the simulations.

To measure the lateral pressure profile in fluorescence experiments, one has to assume that the lateral pressure dominates the excimer/monomer fluorescence ratio. However, our simulation results indicate that the differences in excimer/monomer fluorescence ratios with different acyl chain lengths of di-pyr-PC arise from the differences in internal molecular conformations of di-pyr-PC instead of the lateral pressure profile. This suggests that these probes are not suitable to measure the shape of the lateral pressure profile. However, the probes might still be appropriate to measure how the lateral pressure profile changes at a fixed region in a membrane, when the experiment is carried out in lipid bilayers with different lipid compositions and with a di-pyr-PC probe whose chain length is fixed [15–17,14,18–20].

2. Methods

2.1. Simulation details

We simulated a lipid bilayer composed of 128 DOPC (dioleoylphosphatidylcholine) molecules symmetrically divided into two leaflets. The membrane was fully hydrated by 3655 water molecules. Four randomly chosen DOPC molecules (two in each leaflet) were transformed into DPPC (dipalmitoylphosphatidylcholine) molecules by replacing the double bond region with a saturated one. The DPPC lipids were then used as a basis for pyrene: we attached the pyrene moiety to the 4th, 6th, 8th, or 10th carbon in both hydrocarbon chains of the DPPC molecules, thus creating di-pyr-PCs (see Fig. 1 for a molecular structure). The corresponding systems, in respective order, are denoted as PYR4, PYR6, PYR8, and PYR10. Simulations of the pure DOPC membrane system without pyrene (denoted here as 'DOPC') were also performed for comparison. The choice of these lipids for our simulations is based on the experimental study by Templer et al. [14], as the aim of this work is to study the potential of these probes to measure the lateral pressure profile as suggested by Templer et al. However, the concentration of pyrene-labeled lipids in our simulations (about 3 mol%) is quite a bit larger than that of the concentrations typically used in experiments (about 0.1 mol%). Simulations with a similar number of pyrene-labeled lipids at a concentration of 0.1 mol% would have required about 100 times larger computing resources compared to those used in this work (due to increasing system size). Since the concentration used in our simulations is still quite small, it does not significantly affect the bulk membrane properties [24].

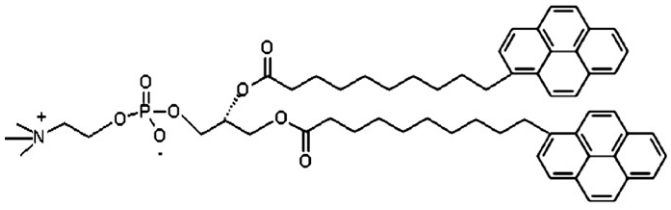

Fig. 1. Chemical structure of di-pyrenyl-phosphatidylcholine (di-pyr-PC) with pyrenes attached to the 10th acyl chain carbon (PYR10).

The parameters for lipids are based on the so-called Berger force field [25], except for the double bonds in DOPC hydrocarbon chains that were taken from Bachar et al. [26]. The general properties of lipid bilayers and acyl chain conformations are well described by the model, with good agreement with experimental data for, e.g., area per molecule and acyl chain order parameters [27,28]. The possible influence of the glycerol and headgroup parameters on our results is discussed in Section 4. For the pyrene moieties in question, we used force field parameters from Ref. [29]. The SPC (single point charge) model was used for water molecules [30]. The atomistic molecular dynamics (MD) simulations were carried out using the GROMACS 4 software package [31] in the NpT ensemble (constant particle number, pressure, and temperature). The temperature and pressure were set to 300 K and 1 bar to match the experimental settings used by Templer et al. [14]. Periodic boundary conditions were used in all three directions. The LINCS algorithm [32] was used to preserve all bond lengths. The time-step used in integrating the equations of motion was chosen to be 2 fs, and the data of the trajectory was saved every 10 ps.

All five systems were equilibrated for 20 ns with temperature and pressure controlled by the semi-isotropic Berendsen algorithm [33] using time constants of 0.1 and 1.0 ps, respectively. In the subsequent production simulations, each lasting for 500 ns, the pressure was controlled by the semi-isotropic Parrinello-Rahman barostat [34] and the temperature by the Nose–Hoover thermostat [35,36] (with no change in time constants). The last 400 ns was used for the analysis. Long-range electrostatic interactions were dealt with the particle mesh Ewald technique [37], with 1 nm real space cut-off. A plain cut-off with a radius of 1.0 nm was used for Lennard–Jones interactions.

We did also simulate di-pyr-PC molecules with each acyl chain length in vacuum. The length of these simulations was 4 μs and simulation parameters were exactly the same as in bilayer simulations, except that the simulation box size was constant and 2 nm plain cut-off was used for the electrostatics.

2.2. Analysis

An excimer is formed when an excited pyrene monomer forms a dimer with a non-excited pyrene monomer. Since this is a quantum-mechanical process, we cannot directly calculate the excimer/monomer fluorescence ratio from the classical simulations. However, we can observe dimers formed by non-excited dimers (see below). Here we analyze the dimer formation rates since in the lateral pressure profile measurement it was assumed that the excimer formation rate dominates the measured excimer/monomer fluorescence ratio [14]. We assume that the dependence of the non-excited dimer formation and the excimer formation rates on external conditions, like pressure and acyl chain length, is similar. In other words, we assume that the essential differences between the formation of a non-excited dimer and an excimer are related to the direct interactions between pyrenes in different states, not to the physical environment around them. Consequently, the dependence of the formation rates for non-excited dimers and excimers on pressure and acyl chain length should be similar, although the actual rates are different.

To analyze the rate of non-excited dimer formation we first divide the simulation trajectory into 1-ns periods. We define that in a given period, two pyrenes in the same molecule are in a dimer state if two conditions are simultaneously satisfied in more than half of the frames: 1) the distance between the centers of mass of the two pyrenes is less than 0.6 nm, and 2) the angle θ between the pyrene planes satisfies the condition $|cos\theta| > 0.9$. Furthermore, different periods in the dimer state are considered to be individual events only if they are separated by a period ≥ 10 ns without dimer states. Finally, the number of individual 1-ns periods where a dimer is formed is calculated for each probe molecule, and the rate is calculated by dividing this number with the simulation length. The 1-ns time periods and the 10-ns lag times were used to ensure that the results are not affected by possible rapid fluctuations between non-excited dimers and monomers. These rapid fluctuations would probably not take place in the excimer formation process since excimers are expected to be more stable than non-excited dimers [38–40]. There is no specific justification for the used numerical values for the length of the period and the lag time. However, repeating the analysis by varying these values by 50% did not change the results essentially. The error bars are based on an 80% confidence interval calculated with the Clopper–Pearson method, assuming that each 1 ns fraction is an independent trial to form a dimer.

In the analysis, we consider only intramolecular dimer formation since in experiments one uses very low di-pyr-PC concentrations to measure lateral pressure, thus intermolecular dimers/excimers are not expected, and specifically the intramolecular excimer formation is assumed to probe the lateral pressure [14,18,20]. However, as in our simulations the probe concentration is higher than that in experiments, there are actually intermolecular dimers present in our simulation [24]. In principle, it is possible that the intermolecular dimer formation competes with the intramolecular dimer formation, thus lowering the rates. Since the total amount of intermolecular dimer events is roughly the same for di-pyr-PC molecules with different acyl chain lengths and the events are relatively rare [24], we expect that those do not affect the results presented in this work.

The pyrenes' density profile $\rho_{pyr}(z)$ and the lateral pressure profile $p(z)$ were computed as a function of z, that is the coordinate along the membrane normal ($z = 0$ corresponding to membrane center). The analysis was made by using standard methods [41,42,13] from the trajectories with removed center of mass motion. Note that the reported lateral pressure profile is $p(z) = (P_{xx}(z) + P_{yy}(z))/2$, instead of $(P_{xx}(z) + P_{yy}(z))/2 - P_{zz}(z)$ since in atomistic models the used methodology produces an unphysical non-constant normal component for the pressure (for further discussion, see [13]).

In the lateral pressure profile measurements with pyrene probes it is assumed that the pyrenes probe the lateral pressure at their locations, though the assumption is not quantitatively formulated [14]. However, a quantitative definition is needed to calculate the pressure at the location of pyrene probes from simulations. Here we assume that the pyrenes gauge the lateral pressure in all locations where it visits during the simulation, however the contribution to the experienced average pressure is less from the locations which are visited more rarely. In practice, this is implemented by calculating the average pressure in the location of pyrenes through the weighting of the pyrenes' density profile:

$$P_{pyr} = \frac{\sum_z \rho_{pyr}(z)p(z)}{\sum_z \rho_{pyr}(z).} \quad (1)$$

3. Results

3.1. Dimer formation

Fig. 2 exemplifies the observations of the dimer formation events. For the demonstration we have picked one PYR4 molecule with only one dimer formation event and one PYR10 with seven dimer formation events during the simulation. The center of mass distance (r) and the cosine of the angle between the planes ($|cos\theta|$) are shown as a function of time for the two pyrenes attached to the same molecule. Also the individual dimerization events are shown. Close to the selected events, the results for r and $|cos\theta|$ are zoomed in to demonstrate the clearly visible dimerization events. This happens at ~247 ns for the event in PYR4 and at ~108.5 ns for the selected event in PYR10. In the example shown for PYR10 the dimer temporarily breaks at ~115 ns, however the reformed dimer is not counted as an individual event due to the 10 ns lag time between individual events (see the Section 2.2). For the same reason, the dimer formation events last always 10 ns after the dimer has been broken.

The calculated dimer formation rates for di-pyr-PC molecules in different environments are shown in Fig. 3. Details about the observed dimerization events in a lipid bilayer are shown in the Supporting Information.

Comparison between the rates in vacuum (Fig. 3a) and in a bilayer (Fig. 3b) shows that the rates are roughly 1.7–3 times larger in vacuum compared to the bilayer environment, however the dependence on the di-pyr-PC acyl chain length is similar in both environments. The generally lower dimerization rates in a bilayer compared to vacuum probably arise from the hindered dynamics [16,17]. Most importantly the results indicate that the bilayer does not affect the acyl chain length dependence on dimer formation rates of di-pyr-PC, thus the chain length dependence is dominated by the molecular conformations of di-pyr-PC instead of the lateral pressure, or other bilayer properties.

Experimental estimates for the excimer formation rates in a bilayer are roughly 0.1 $(ns)^{-1}$ and 0.05 $(ns)^{-1}$ for PYR4 and PYR10, respectively [16]. The experimental numbers are larger than the dimer formation rate values 0.003 $(ns)^{-1}$ and 0.01 $(ns)^{-1}$ calculated from simulations for PYR4 and PYR10 in a lipid bilayer, respectively. This is not surprising since the non-excited dimer formation in a classical model is a different process than the quantum-mechanical excimer formation.

The excimer/monomer fluorescence intensity ratios measured by Templer et al. [14]. for different di-pyr-PC molecules are shown in Fig. 3c. Assuming that the acyl chain length dependence of excimer/monomer fluorescence ratio and dimer formation rate in di-pyr-PC molecules are determined by the physical environment, the relative differences between different molecules in Fig. 3b and c should be similar. However, we observe that the relative dimer formation rate is lower for PYR4 and higher for PYR10 compared to the measured excimer/monomer fluorescence ratios. This is in line with the above comparison between simulated dimer and measured excimer formation rates, since the difference was larger for PYR4 than for PYR10.

3.2. Lateral pressure in the location of pyrene probes

The lateral pressure profiles for membranes containing di-pyr-PCs with different acyl chain lengths are shown in Fig. 4a, and the density profiles of pyrenes are shown in Fig. 4b. As expected, the low concentration of probes does not have significant effects on the lateral pressure profile, and the density of pyrene probes moves towards the center of the bilayer for increasing acyl chain length in good agreement with experiments [43].

The average lateral pressure in the location where pyrenes reside, P_{pyr}, calculated with Eq. (1), is shown in Fig. 5. In contrast to the calculated pyrene dimer formation rates and the measured excimer/monomer fluorescence ratios, the average lateral pressure in the locations of the pyrenes decreases monotonously towards the bilayer center.

4. Discussion

Templer et al. suggested that the measured pyrene excimer/monomer fluorescence ratio reports the relative lateral pressure in the location of pyrenes inside a lipid bilayer [14]. Following this argument (Fig. 3c), the

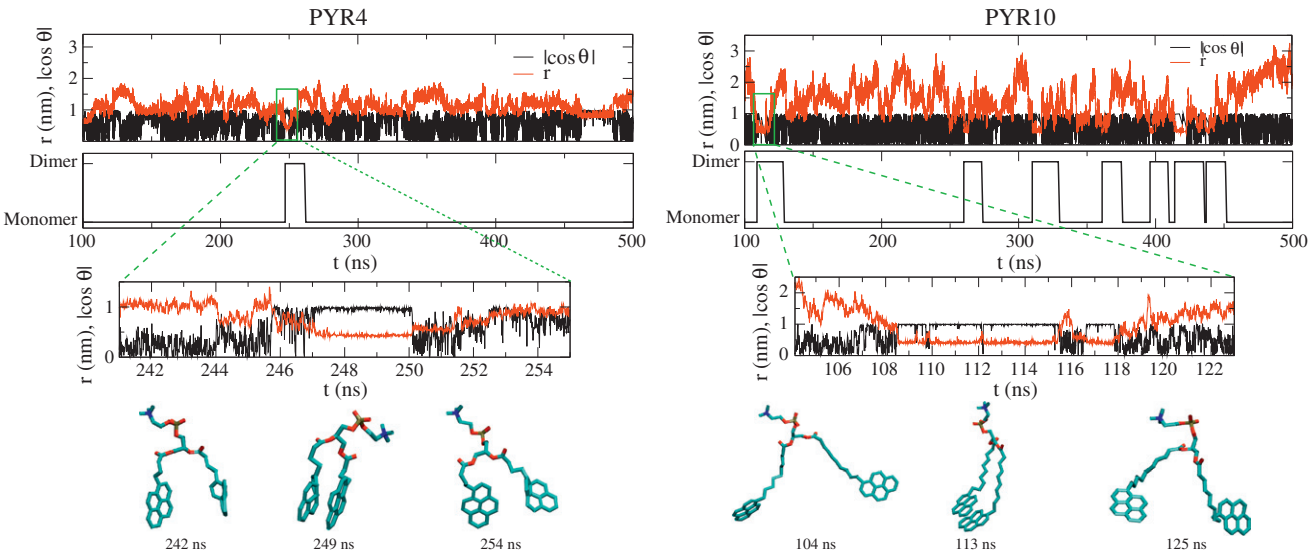

Fig. 2. The dimer formation analysis exemplified for the selected PYR4 (left column) and PYR10 (right column) molecules embedded into a bilayer. First row: (black) Cosine of the angle between pyrene planes, $|cos\theta|$, and (red) the center of mass distance, r, between pyrenes attached to the same di-pyr-PC molecule as a function of time. Second row: The observed individual dimer formation events. Third row: An inset zooming in to the data for $|cos\theta|$ and r close to the selected dimerization events. Fourth row: Example conformations for di-pyr-PC from the simulation before, during, and after dimer formation (other lipids and water not shown for clarity).

pressure would first decrease from the location of PYR4 to the location of PYR8 and then increase as one moves closer to the membrane center where PYR10 is located. The pressure increase from PYR8 to PYR10 was not expected at the time when the original experiment was done [14,44], however it seems to agree with more recent molecular dynamics simulation results where the central maximum of the pressure profile has been observed in several independent studies [12,13]. Some authors (including some of us) have concluded that this represents good agreement between experimental and theoretical results [12,13,45].

However, a more careful comparison between experimental results and simulations reveals that the solution is not that straightforward. According to the underlying assumption that is used to interpret the lateral pressure profile measurements by Templer et al. [14], the pressure is the main regulator of the acyl chain length dependence of dimer formation rates. However, comparison between Fig. 3a and b shows that in our simulations the acyl chain length dependence of dimerization rate is similar in vacuum and bilayer environments. This result indicates that the acyl chain length dependence of dimer formation rates is dominated by the internal conformations of di-pyr-PC molecules.

On the other hand, according to the assumptions used to interpret the lateral pressure profile measurements by Templer et al. [14], the excimer/monomer fluorescence ratio would mainly depend on the excimer formation rate which would, in turn, be determined by the lateral pressure. The assumption that the lateral pressure dominates the relative excimer formation rate indicates that also the dimer formation rate should be determined by the lateral pressure. However, from Fig. 5 we see that the pressure decreases monotonously from the location of PYR4 to the location of PYR10, while the dimer formation rate is roughly constant from PYR4 to PYR6 but significantly higher for PYR10. We suggest that the there is no correlation between the lateral pressure and the relative dimerization rates, or that the correlation is weak, since the latter is mainly determined by the conformations of di-pyr-PC molecules.

The assumptions in the lateral pressure profile measurement would also indicate that the excimer/monomer ratio and the dimerization rate would have similar dependence on acyl chain length. However, comparison between Fig. 3b and c reveals that the chain length dependence of dimer formation rates in simulations and the excimer/monomer fluorescence ratios in experiments are not exactly similar. Particularly, the

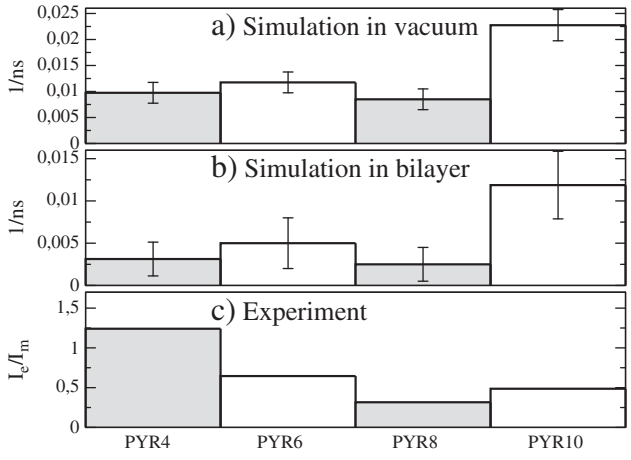

Fig. 3. Non-excited dimer formation rates for different di-pyr-PCs calculated from simulations in a) vacuum and in b) a bilayer. c) Measured excimer/monomer fluorescence intensity by Templer et al. [14].

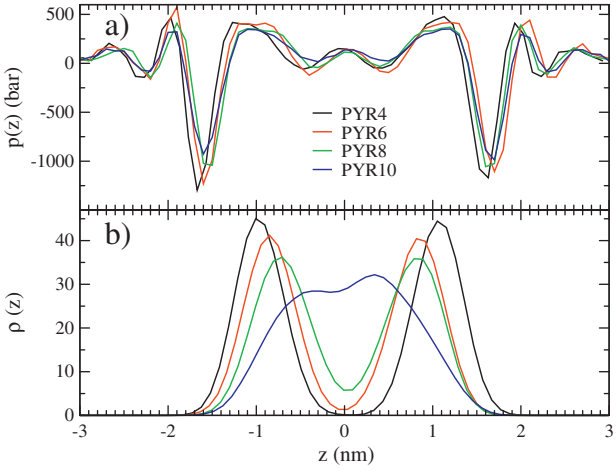

Fig. 4. a) Lateral pressure profiles calculated from MD simulations for membranes containing different di-pyr-PCs. b) Density distributions of pyrene moieties of di-pyr-PCs. The value $z = 0$ corresponds to membrane center.

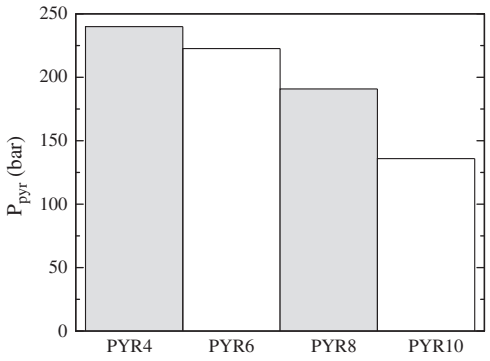

Fig. 5. Average lateral pressure in the location of pyrenes calculated from MD simulations.

simulations predict a relatively too low rate for PYR4 and a too high rate for PYR10. Possible reasons for this are that the excimer/monomer ratio is not solely determined by physical environment, or that the di-pyr-PC properties are not correctly described by the used model. First, in the work by Templer et al. and in the subsequent discussion [14], the possible influence of oxygen quenching on the results is discussed. Templer et al. report that the amount of oxygen in the sample did not affect the PYR4 results, however the di-pyr-PC molecules with longer acyl chains were not studied. In more recent experimental and theoretical studies oxygen has been found to preferentially locate in the membrane center [46,47], thus it is very well possible that the longer acyl chain di-pyr-PC molecules would be more strongly quenched than PYR4. In this case, the acyl chain dependence of the excimer/monomer ratio would strongly depend on the level of quenching and not only on the physical environment. Second, regarding the quality of the simulation model, the most relevant parts are the acyl chains since pyrene probes are located and form dimers in the hydrophobic region of the bilayer. The used simulation model has been shown to model this part of the lipid bilayer with good accuracy [27,28]. Especially the acyl chains most likely sample the correct conformations since the acyl chain C – H order parameters are in very good agreement with experiments. However, the excimer formation has been suggested to depend on subtle details of the molecular conformations close to the glycerol region [48], which would also apply to the dimer formation. Hence, while there is a lot of support for the validity of the used simulation model in acyl chain region, we cannot fully exclude the possibility that the inaccuracies in the used model in the glycerol region [49,28,50,51] would affect the observed dimerization rates. In conclusion, to fully explain the differences in the chain length dependence between dimer formation rates in simulations, and the excimer/monomer fluorescence ratios in experiments would a require significant effort, including measurements to study the possible oxygen quenching and a possible re-parameterization of the model. These studies are beyond the scope of this work.

In spite of the above discussed differences, the qualitative increase from PYR8 to PYR10 is seen in all the results shown in Fig. 3, i.e. in simulated dimer formation rates in vacuum and in a bilayer, and also in excimer/monomer fluorescence intensities measured by Templer et al. [14]. From this we conclude that the observed increases in the rate from PYR8 to PYR10 originate from the conformational differences, not from the increase in lateral pressure.

Summarizing, all the observations indicate that the acyl chain length dependence of dimer formation rate is not determined by the lateral pressure, instead the dominant contributions are the conformational differences of the molecules.

Finally, the present work highlights that one can clearly characterize dimer formation events using classical simulations as demonstrated in Fig. 2 and also pointed out by other authors [52]. This is quite remarkable and indicates that classical atomistic simulations have potential for interpretation of pyrene fluorescence experiments.

5. Conclusions

According to the assumptions used to measure the shape of the lateral pressure profile using di-pyr-PC probes, the relative excimer/monomer fluorescence ratio between di-pyr-PCs with different acyl chain lengths is related to the excimer formation rate, which is determined by the lateral pressure [14]. Accordingly, the relative dimer formation rates between di-pyr-PCs with different acyl chain lengths should be determined by the lateral pressure. However, based on our simulation results the acyl chain length dependence of dimer formation rates is not determined by the lateral pressure, instead it is dominated by the conformations of di-pyr-PC molecules. Therefore, the results of this work do not support the usage of di-pyr-PC probes for the measurements of the shape of the lateral pressure profile.

However, the measurements of the changes in the lateral pressure profile are potentially better justified [21]. If the di-pyr-PC with a fixed acyl chain length is embedded into bilayers with different lipid composition, the probe may provide relevant information of changes in the lateral pressure profile [15–17,14,18–20], assuming that the pyrenes reside largely in the same membrane region regardless of the bilayer system studied.

Acknowledgements

Paavo Kinnunen is acknowledged for useful discussions. OHSO acknowledges the Emil Aaltonen foundation for the financial support. MF and IV thank the Academy of Finland (project funding and the Center of Excellence scheme) and the European Research Council (Advanced Grant CROWDED-PRO-LIPIDS) for the financial support. CSC — IT Centre for Finland (Espoo) and the HorseShoe cluster (Odense, Denmark) are acknowledged for computational resources.

Appendix A. Supplementary data

Supplementary data to this article can be found online at http://dx.doi.org/10.1016/j.bbamem.2014.01.030.

References

[1] U. Seifert, R. Lipowsky, Structure and Dynamics of Membranes, Elsevier, Amsterdam, 1995. 403–463.
[2] T.J. McIntosh, S.A. Simon, Title, Annu. Rev. Biophys. Biomol. Struct. 35 (2006) 177.
[3] A.G. Lee, How lipids affect the activities of integral membrane proteins, Biochim. Biophys. Acta 1666 (2004) 62–87.
[4] A. Ben-Shaul, I. Szleifer, W.M. Gelbart, Statistical thermodynamics of amphiphile chains in micelles, Proc. Natl. Acad. Sci. U. S. A. 81 (1984) 4601–4605.
[5] S.A. Safran, Statistical Thermodynamics of Surfaces, Interfaces, and Membranes, Addison-Wesley, Reading, MA, 1994.
[6] R.S. Cantor, Lateral pressures in cell membranes: a mechanism of modulation of protein function, J. Phys. Chem. B 101 (1997) 1723–1725.
[7] D. Marsh, Lateral pressure profile, spontaneous curvature frustration, and the incorporation and conformation of proteins in membranes, Biophys. J. 93 (2007) 3884–3899.
[8] O.H.S. Ollila, M. Louhivuori, S. Marrink, I. Vattulainen, Protein shape change has a major effect on the gating energy of a mechanosensitive channel, Biophys. J. 100 (2011) 1651–1659.
[9] S.M. Oversteegen, F.A.M. Leermakers, Thermodynamics and mechanics of bilayer membranes, Phys. Rev. E. 62 (2000) 8453–8461.
[10] M. Hu, D.H. de Jong, S.J. Marrink, M. Deserno, Gaussian curvature elasticity determined from global shape transformations and local stress distributions: a comparative study using the martini model, Faraday Discuss. 161 (2013) 365–382.
[11] S.H. White, Biophysical dissection of membrane proteins, Nature 459 (2009) 344–346.
[12] O.H.S. Ollila, I. Vattulainen, Lateral Pressure Profiles in Lipid Membranes: Dependence on Molecular Composition, in: M. Sansom, P. Biggin (Eds.), Molecular Simulations and Biomembranes: From Biophysics to Function, Royal Society of Chemistry, 2010, pp. 26–55.
[13] O.H.S. Ollila, Lateral Pressure in Lipid Membranes and Its Role in Function of Membrane Proteins, (Ph.D. thesis) Tampere University of Technology, 2010.
[14] R.H. Templer, S.J. Castle, A.R. Curran, G. Rumbles, D.R. Klug, Sensing isothermal changes in the lateral pressure profile in model membranes using di-pyrenol phosphatidylcholine, Faraday Discuss. 111 (1998) 41–53.

[15] T. Thuren, J.A. Virtanen, P.K. Kinnunen, Estimation of the equilibrium lateral pressure in 1-palmitoyl-2-[6(pyren-1-yl)]hexanoyl-glycerophospholipid liposomes, Chem. Phys. Lipids 41 (1986) 329–334.
[16] K. Cheng, L. Ruymgaart, L. Liu, P. Somerharju, I. Sugar, Intramolecular excimer kinetics of fluorescent dipyrenyl lipids: 2. dope/dopc membranes, Biophys. J. 67 (1994) 914–921.
[17] K. Cheng, L. Ruymgaart, L. Liu, P. Somerharju, I. Sugar, Intramolecular excimer kinetics of fluorescent dipyrenyl lipids: 1. dmpc/cholesterol membranes, Biophys. J. 67 (1994) 902–913.
[18] T. Kamo, M. Nakano, Y. Kuroda, T. Handa, Effects of an amphipathic α-helical peptide on lateral pressure and water penetration in phosphatidylcholine and monoolein mixed membranes, J. Phys. Chem. B 110 (2006) 24987–24992.
[19] T. Kamo, T. Handa, M. Nakano, Lateral pressure change on phase transitions of phosphatidylcholine/diolein mixed membranes, Colloids Surf. B: Biointerfaces 104 (2013) 128–132.
[20] T.N. Murugova, M. Klacsova, P. Pullmannova, J. Karlovska, P. Balgavy, Study of interaction of long-chain n-alcohols with fluid dopc bilayers by a lateral pressure sensitive fluorescence probe, Gen. Physiol. Biophys. 131 (2012) 225–227.
[21] J. Lehtonen, P. Kinnunen, Changes in the lipid dynamics of liposomal membranes induced by poly(ethylene glycol): free volume alterations revealed by inter- and intramolecular excimer-forming phospholipid analogs, Biophys. J. 66 (1994) 1981–1990.
[22] M. Sassaroli, M. Vauhkonen, P. Somerharju, S. Scarlata, Dipyrenylphosphatidylcholines as membrane fluidity probes. Pressure and temperature dependence of the intramolecular excimer formation rate, Biophys. J. 64 (1993) 137–149.
[23] K. Cheng, P. Somerharju, Effects of unsaturation and curvature on the transverse distribution of intramolecular dynamics of dipyrenyl lipids, Biophys. J. 70 (1996) 2287–2298.
[24] M.D. Franovà, J. Repàkovà, J.M. Holopainen, I. Vattulainen, How to link pyrene to its host lipid to minimize the extent of membrane perturbations and to optimize pyrene dimer formation, Chem. Phys. Lipids 177 (2014) 19–25.
[25] O. Berger, O. Edholm, F. Jähnig, Molecular dynamics simulations of a fluid bilayer of dipalmitoylphosphatidylcholine at full hydration, constant pressure, and constant temperature, Biophys. J. 72 (1997) 2002–2013.
[26] M. Bachar, P. Brunelle, D.P. Tieleman, A. Rauk, Molecular dynamics simulation of a polyunsaturated lipid bilayer susceptible to lipid peroxidation, J. Phys. Chem. B 108 (2004) 7170–7179.
[27] S. Ollila, M.T. Hyvönen, I. Vattulainen, Polyunsaturation in lipid membranes: dynamic properties and lateral pressure profiles, J. Phys. Chem. B 111 (2007) 3139–3150.
[28] T.M. Ferreira, F. Coreta-Gomes, O.H.S. Ollila, M.J. Moreno, W.L.C. Vaz, D. Topgaard, Cholesterol and popc segmental order parameters in lipid membranes: solid state ^{1}H-^{13}C NMR and MD simulation studies, Phys. Chem. Chem. Phys. 15 (2013) 1976–1989.
[29] J. Repàkovà, J.M. Holopainen, M. Karttunen, I. Vattulainen, Influence of pyrene-labeling on fluid lipid membranes, J. Phys. Chem. B 110 (2006) 15403–15410.
[30] H.J.C. Berendsen, J.P.M. Postma, W.F. van Gunsteren, J. Hermans, Intermolecular Forces, Reidel, Dordrecht, 1981. 331–342.
[31] B. Hess, C. Kutzner, D. van der Spoel, E. Lindahl, Gromacs 4: algorithms for highly efficient, load-balanced, and scalable molecular simulation, J. Chem. Theory Comput. 4 (2008) 435–447.
[32] B. Hess, H. Bekker, H.J.C. Berendsen, J.G.E.M. Fraaije, LINCS: a linear constraint solver for molecular dynamics simulations, J. Comput. Chem. 18 (1997) 1463–1472.
[33] H.J.C. Berendsen, J.P.M. Postma, W.F. van Gunsteren, A. DiNola, J.R. Haak, Molecular dynamics with coupling to an external bath, J. Chem. Phys. 81 (1984) 3684–3690.
[34] M. Parrinello, A. Rahman, Polymorphic transitions in single crystals: a new molecular dynamics method, J. Appl. Phys. 52 (1981) 7182–7190.
[35] S. Nose, A molecular dynamics method for simulations in the canonical ensemble, Mol. Phys. 52 (1984) 255–268.
[36] W.G. Hoover, Canonical dynamics: equilibrium phase-space distributions, Phys. Rev. A 31 (1985) 1695–1697.
[37] U.L. Essman, M.L. Perera, M.L. Berkowitz, T. Larden, H. Lee, L.G. Pedersen, A smooth particle mesh Ewald potential, J. Chem. Phys. 103 (1995) 8577–8592.
[38] A. Warshel, E. Huler, Theoretical evaluation of potential surfaces, equilibrium geometries and vibronic transition intensities of excimers: the pyrene crystal excimer, Chem. Phys. 6 (1974) 463–468.
[39] F.M. Winnik, Photophysics of preassociated pyrenes in aqueous polymer solutions and in other organized media, Chem. Rev. 93 (1993) 587–614.
[40] O. Khakhel', Absorption spectra of pyrene aggregates in saturated solutions, J. Appl. Spectrosc. 68 (2001) 280–286.
[41] D.V. der Spoel, E. Lindahl, B. Hess, A.R. van Buuren, E.A.P.J. Meulenhoff, D.P. Tieleman, A.L.T.M. Sijbers, K.A. Feenstra, R. van Drunen, H.J.C. Berendsen, GROMACS user manual version 4.0, www.gromacs.org 2005.
[42] O.H.S. Ollila, H.J. Risselada, M. Louhivuori, E. Lindahl, I. Vattulainen, S.J. Marrink, 3d pressure field in lipid membranes and membrane-protein complexes, Phys. Rev. Lett. 102 (2009) 078101.
[43] M. Sassaroli, M. Ruonala, J. Virtanen, M. Vauhkonen, P. Somerharju, Transversal distribution of acyl-linked pyrene moieties in liquid-crystalline phosphatidylcholine bilayers. A fluorescence quenching study, Biochemistry 34 (1995) 8843–8851.
[44] I. Szleifer, A. Ben-Shaul, W.M. Gelbart, Chain packing statistics and thermodynamics of amphiphile monolayers, J. Phys. Chem. 94 (1990) 5081–5089.
[45] M. Orsi, D.Y. Haubertin, W.E. Sanderson, J.W. Essex, A quantitative coarse-grain model for lipid bilayers, J. Phys. Chem. B 112 (2008) 802–815.
[46] M.S. Al-Abdul-Wahid, C.-H. Yu, I. Batruch, F. Evanics, R. Pomès, R.S. Prosser, A combined NMR and molecular dynamics study of the transmembrane solubility and diffusion rate profile of dioxygen in lipid bilayers, Biochemistry 45 (2006) 10719–10728.
[47] R.M. Cordeiro, Reactive oxygen species at phospholipid bilayers: distribution, mobility and permeation, Biochim. Biophys. Acta 1838 (2014) 438–444.
[48] K.K. Eklund, J.A. Virtanen, P.K.J. Kinnunen, J. Kasurinen, P.J. Somerharju, Conformation of phosphatidylcholine in neat and cholesterol-containing liquid-crystalline bilayers. Application of a novel method, Biochemistry 31 (1992) 8560–8565.
[49] P. Prakash, R. Sankararamakrishnan, Force field dependence of phospholipid headgroup and acyl chain properties: comparative molecular dynamics simulations of dmpc bilayers, J. Comput. Chem. 31 (2010) 266–277.
[50] T.M. Ferreira, Structure and Dynamics in Amphiphilic Bilayers: NMR and MD Simulation Studies, (Ph.D. thesis) Lund University, 2013.
[51] O.H.S. Ollila, Response of the hydrophilic part of lipid membranes to changing conditions - a critical comparison of simulations to experiments, http://arxiv.org/abs/1309.2131 2013.
[52] H. Yan, P. Cui, C.-B. Liu, S.-L. Yuan, Molecular dynamics simulation of pyrene solubilized in a sodium dodecyl sulfate micelle, Langmuir 28 (2012) 4931–4938.